VOLUME 123, NUMBER 30
AUGUST 1, 2001

JOURNAL OF THE AMERICAN CHEMICAL SOCIETY

Viscosity Effects on the Thermal Decomposition of Bis(perfluoro-2-*N*-propoxypropionyl) Peroxide in Dense Carbon Dioxide and Fluorinated Solvents

W. Clayton Bunyard,[†] John F. Kadla,*[,‡] and Joseph M. DeSimone*

Contribution from the National Science Foundation Science and Technology Center for Environmentally Responsible Solvents and Processes, Department of Chemistry, University of North Carolina at Chapel Hill, CB 3290, Chapel Hill, North Carolina 27599-3290

Received February 6, 2001

Abstract: The thermal decomposition of the free-radical initiator bis(perfluoro-2-*N*-propoxyprionyl) peroxide (BPPP) was studied in dense carbon dioxide and a series of fluorinated solvents. For the fluorinated solvents, the observed first-order decomposition rate constants, k_{obs}, increased with decreasing solvent viscosity, suggesting a single-bond decomposition mechanism. The k_{obs} values are comparatively larger in dense carbon dioxide and similar to the "zero-viscosity" rate constants extrapolated from the decomposition kinetics in the fluorinated solvents. The decomposition activation parameters demonstrate a compensation behavior of the activation enthalpy with the activation entropy upon change in solvent viscosity. Comparison of the change in activation parameter values upon change in solvent viscosity for BPPP with two additional initiators, acetyl peroxide (AP) and trifluoroacetyl peroxide (TFAP), further suggests that carbon dioxide exerts a very minimal influence on the decomposition mechanism of these initiators through solvent-cage effects.

Introduction

In recent years there has been great interest in the use of supercritical fluids (SCFs) as solvents for chemical reactions due to their tunable solvent properties. Carbon dioxide is an especially attractive SCF as it is naturally occurring, readily available, and has an easily accessible critical point of T_c = 31.1 °C and P_c = 73.8 bar. While demonstrating applicability in varied fields of chemistry,[1] CO_2 has shown particular utility as a solvent for conducting free-radical chain reactions, as it is effectively inert to free radicals. The study of free-radical polymerizations has been prolific in dense carbon dioxide in the form of solution, precipitation, and dispersion polymerizations.[2] A number of studies have focused on determining if CO_2 exerts any unique solvent effects on these polymerizations through examination of the various steps of the polymerization process such as initiation,[3−5] propagation,[6−8] and termination.[9]

* To whom correspondence should be addressed.
[†] Present address: Kimberly-Clark Corporation, Neenah, WI.
[‡] Present address: College of Natural Resources, North Carolina State University.

(1) The reader is referred to *Chem. Rev.* **1999**, *99*, 9 (2) which contains several pertinent reviews on this subject.

(2) Kendall, J. L.; Canelas, D. A.; Young, J. L.; DeSimone, J. M. *Chem. Rev.* **1999**, *99*, 543.

(3) DeSimone, J. M.; Guan, Z.; Eisbernd, C. S. *Science* **1992**, *257*, 945.

(4) Guan, Z.; Combes, J. R.; Menceloglu, Y. Z.; DeSimone, J. M. *Macromolecules* **1993**, *26*, 2663.

(5) Dessipri, E.; Hsiao, Y. L.; Juventin Mathes, A. C.; Shaffer, K. A.; DeSimone, J. M. *Polym. Mater. Sci. Eng.* **1996**.

(6) van Herk, A. M.; Manders, B. G.; Canelas, D. A.; Quadir, M. A.; DeSimone, J. M. *Macromolecules* **1997**, *30*, 4780.

(7) Beuermann, S.; Buback, M.; Schmaltz, C. *Macromolecules* **1998**, *31*, 8069.

(8) Quadir, M. A.; DeSimone, J. M.; van Herk, A. M.; German, A. L. *Macromolecules* **1998**, *31*, 6481.

(9) Beuermann, S.; Buback, M.; Schmaltz, C. *Ind. Eng. Chem. Res.* **1999**, *38*, 3338.

10.1021/ja0103344 CCC: $20.00
Published on Web 07/03/2001

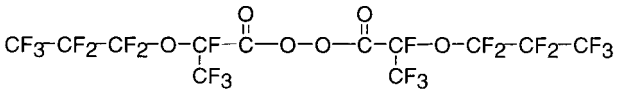

Figure 1. Structure of bis(perfluoro-2-*N*-propoxypropionyl) peroxide, BPPP.

A seminal example involves the report of the decomposition kinetics and initiator efficiency of the ubiquitous free-radical initiator 2,2′-azobis(isobutyronitrile) (AIBN) in CO_2.[3,4] Using product analysis and spectroscopic studies, it was revealed that supercritical CO_2 was effectively inert to such free-radical reactions. The decomposition rate of AIBN was 2.5 times slower in CO_2 than in benzene, attributable to the low dielectric constant of CO_2. Using radical scavenging methods, high radical initiator efficiencies of greater than 80% were observed due to negligible solvent cage effects in the low viscosity CO_2 medium. Since the initial report, AIBN has been used for free-radical polymerizations of a variety of monomers such as styrenics and (meth)acrylates in dense CO_2.[2]

While AIBN is a useful initiator for hydrocarbon monomers, perfluorinated diacyl peroxides (PDPs) are more suitable initiators for the polymerization of fluoroolefins, such as tetrafluoroethylene (TFE), where it produces thermally stable polymer endgroups.[10] The successful use of the fluorinated diacyl peroxide, bis(perfluoro-2-*N*-propoxypropionyl) peroxide (BPPP) (Figure 1) as an initiator for copolymerizations of TFE in CO_2 has been reported by Romack et al.[11] However, the detailed decomposition kinetics for BPPP in CO_2 has yet to be studied. Further advances in the area of fluoroolefin polymerization in CO_2, such as the development of continuous polymerization processes,[12] require the knowledge of the decomposition kinetics of appropriate initiators such as BPPP.

The study herein focuses on the determination of the homolytic decomposition mechanism for BPPP and the influence of dense carbon dioxide on its decomposition kinetics.

Results and Discussion

Decomposition Kinetics. The dramatic influence of fluorination on the decomposition kinetics of diacyl peroxides has been shown by the early studies of Novikov[13] and Zhao,[14] with the PDPs having activation enthalpies typically 5−8 kcal/mol lower than the nonfluorinated analogues. Through use of molecular orbital calculations, Sawada[15] discovered that fluorination results in an increase in the dihedral angle between the COO planes and a decrease in covalency of the peroxy O−O bond and the C−C bond between the fluoroalkyl chain and the carbonyl carbon. Increasing the length of the fluoroalkyl chains further destabilizes these bonds, leading to an increase in decomposition rate with increasing fluoroalkyl chain length. While the structural dependence on PDP decomposition kinetics has been studied extensively, the solvent dependence has not been explored. Further, the mechanism of PDP bond homolysis is unclear.

The kinetic studies for BPPP decomposition were conducted in the temperature range of 20−45 °C. In situ FTIR provided a useful method for monitoring the thermal decomposition of the diacyl peroxides under study due to the strong symmetric and asymmetric stretches of the acyl peroxide groups. A typical FTIR absorbance difference spectral series for the thermal decomposition of BPPP in CO_2 illustrating the decrease in peroxide absorbance with time is shown in Figure 2. At the lower frequency side of the peroxide doublet is the growing absorbance of a radical decomposition product, CF_3COF (1882 cm^{-1}).

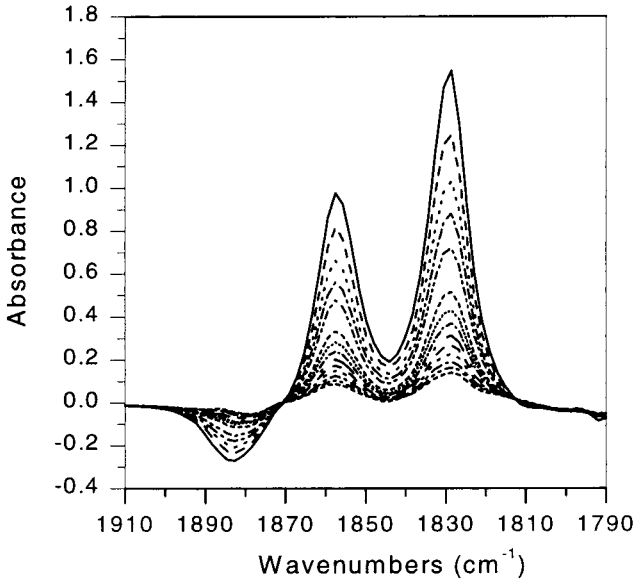

Figure 2. Time-resolved FTIR difference spectra for thermal decomposition of BPPP in CO_2 taken at an interval of 900 s at 30 °C.

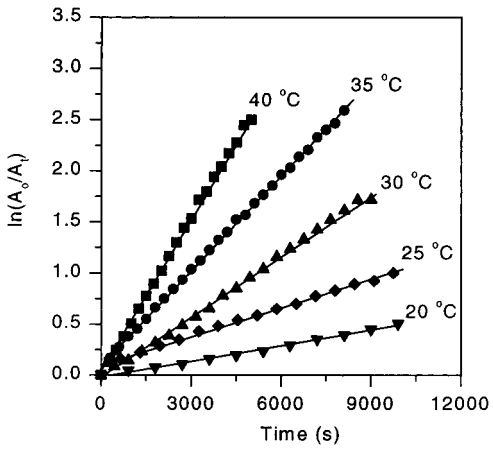

Figure 3. First-order kinetic analysis for thermal decomposition of BPPP in CO_2 (ρ = 0.87 g/mL) at $[BPPP]_o$ = 0.03 M.

Application of first-order kinetic analysis to the decomposition data yields linear plots of $\ln(A_o/A_t)$ versus time as illustrated in Figure 3 for BPPP decomposition in CO_2 at a density of 0.87 g/mL. The data clearly follows a first-order rate law at all temperatures, consistent with the work of Zhao[14] and Novikov[13] for BPPP thermal decomposition in $CF_2ClCFCl_2$. Initial peroxide concentrations ranged between 0.005 and 0.03 M, with no observable influence of peroxide concentration on the decomposition kinetics. Under all conditions investigated, no deviation from first-order kinetics was observed in any of the reaction media tested. Moreover, reactions employing radical scavengers (data not shown) showed no effect on the degradation kinetics, indicating minimal contribution from induced decomposition processes.

The observed first-order rate constants, k_{obs}, extracted from the kinetic analysis for the thermal decomposition in the various

(10) Hintzer, K.; Lohr, G. In *Modern Fluoropolymers*; Scheirs, J., Ed.; John Wiley & Sons: Chichester, 1997; pp 223−237.
(11) Romack, T. J.; Treat, T. A.; DeSimone, J. M. *Macromolecules* **1995**, *28*, 8429.
(12) Charpentier, P. A.; Kennedy, K. A.; DeSimone, J. M.; Roberts, G. W. *Macromolecules* **1999**, *32*, 5973.
(13) Novikov, V. A.; Sass, V. P.; Ivanova, L. S.; Sokolov, L. F.; Sokolov, S. V. *Vysokomol. Soyed.* **1975**, *A17*, 1235.
(14) Zhao, C.; Zhou, R.; Pan, H.; Jin, X.; Qu, Y.; Wu, C.; Jiang, X. *J. Org. Chem.* **1982**, *47*, 2009.
(15) Sawada, H.; Nakayama, M. *J. Fluorine Chem.* **1990**, *50*, 393.

Table 1. Observed First-order Rate Constants for Thermal Decomposition of BPPP in Fluorinated Solvents and Dense Carbon Dioxide

	$k_{obs} \times 10^5$ (s^{-1})						
temp (°C)	CO_2 (0.78)[a]	CO_2 (0.87)[a]	CO_2 (0.98)[a]	$CFCl_3$	$CF_2ClCFCl_2$	$C_6F_{12}O_2$	$C_{15}F_{30}O_5$
20	5.00 ± 0.1	5.30 ± 0.08	5.30 ± 0.1	4.16 ± 0.16	3.39 ± 0.1	2.64 ± 0.08	1.24 ± 0.04
25	9.00 ± 0.1	10.7 ± 0.3	9.60 ± 0.2	8.65 ± 0.3	6.50 ± 0.4	6.05 ± 0.3	3.00 ± 0.05
30	15.8 ± 0.2	15.8 ± 0.6	15.9 ± 0.4	14.7 ± 0.6	13.9 ± 0.6	9.75 ± 0.5	8.85 ± 1.0
35	20.0 ± 1.1	28.8 ± 1.9	28.4 ± 1.6	27.1 ± 1.1	25.4 ± 1.4	22.0 ± 0.6	28.0 ± 1.9
40	47.0 ± 2.9	52.0 ± 3.1	54.0 ± 2.5	55.2 ± 2.8	48.0 ± 2.4	44.9 ± 1.7	47.0 ± 3.4

[a] Density in g/mL.

Scheme 1. Kinetically Important Steps of the (a) Multiple-Bond and (b) Single-Bond Decomposition Pathways for the Thermal Decomposition of BPPP

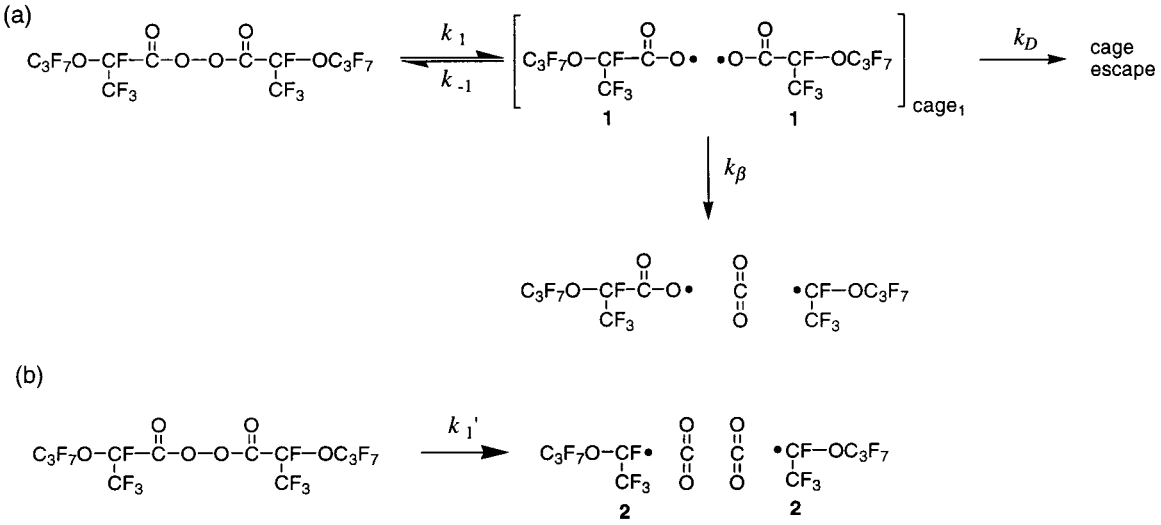

solvents are listed in Table 1. In all cases, the error in the rate coefficients varied with temperature but was approximately ±7%. The k_{obs} values show the expected increase with increasing temperature but also show a dependence upon solvent ranging in magnitude by a factor of 4.

It is well established in the literature that diacyl peroxides can homolytically decompose by either a one-bond mechanism to produce a geminate carboxy radical pair or by a concerted multiple-bond mechanism to produce a geminate alkyl radical pair and two molecules of CO_2.[16] The latter mechanism is typically favored with increasing stability of the forming alkyl radical. However, due to the influence of the reaction medium, further mechanistic complexity is introduced into the single-bond decomposition pathway. These two decomposition pathways for BPPP are illustrated in Scheme 1 with the rate constants assigned to the steps which have direct consequence on the rate of decomposition. Some notable examples of experimental tools utilized to distinguish between single-bond and multiple-bond decomposition mechanisms include use of ^{18}O-label scrambling methods, variation of solvent viscosity, and detailed product analyses.[16] Other reaction medium properties such as dielectric constant and internal pressure can influence the decomposition kinetics,[17] but these are not necessarily helpful for distinguishing between single-bond and multiple-bond homolysis mechanisms. For BPPP, the study of solvent viscosity effects on k_{obs} and decomposition product analysis are the most experimentally accessible methods due to its low thermal stability at near ambient temperatures.

(16) Fujimori, K. In *Organic Peroxides*; Ando, W., Ed.; John Wiley & Sons Ltd.: New York, 1992; pp 319−386.

(17) Tanko, J. M.; Suleman, N. K. In *Energetics of Organic Free Radicals*; Simoes, J. A. M., Greenberg, A., Liebman, J. F., Eds.; Blackie Academic & Professional: New York, 1996; p 224.

Influence of Solvent Viscosity on Decomposition Kinetics. According to the solvent cage concept the decomposition rate of a one-bond initiator should be dependent upon the viscosity (η) of the reaction medium. Decomposition of BPPP by a single-bond decomposition mechanism is illustrated in Scheme 1a, where O−O bond cleavage produces an initial geminate carboxyl radical pair. The rate of diffusion of this radical pair is governed by the viscosity of the surrounding medium. As the viscosity of the medium increases, the probability of cage return to reform the initial diacyl peroxide increases, resulting in a decrease in the observed rate of peroxide decomposition. The existence of competing reactions such as decarboxylation acts to decrease the probability of cage return and thereby increases the observed decomposition rate. Thus, the observed decomposition rate constant k_{obs} (eq 1) is a composite of the rate constants: k_1 for bond homolysis, k_{-1} for cage return, k_D for diffusion of the geminate radicals, and k_β for β-scission processes that may compete with diffusion and cage return (i.e., decarboxylation).

$$k_{obs} = \frac{k_1(k_D + k_\beta)}{k_{-1} + k_D + k_\beta} \quad (1)$$

Conversely, for the multiple-bond decomposition mechanism depicted in Scheme 1b, the degradation kinetics should be insensitive to the viscosity of the medium. This is due to the statistical improbability of reforming three bonds in the solvent cage ($k_{-1} = 0$). In this case, k_{obs} is defined simply by eq 2 as a rate constant for bond homolysis, k_1'.

$$k_{obs} = k_1' \quad (2)$$

It must be said however, that the lack of a solvent viscosity

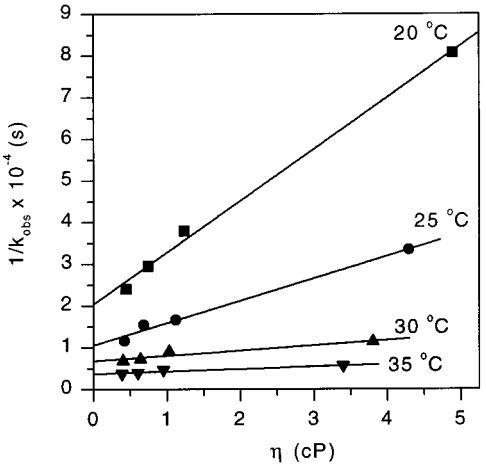

Figure 4. Solvent viscosity and temperature dependence of k_{obs} for BPPP thermal decomposition in fluorinated solvents.

effect on the decomposition rate does not necessarily preclude a one-bond scission mechanism. No viscosity effect would be observed in the case where k_β is much greater than both k_D and k_{-1} as the β-scission pathway would consume the predominance of the carboxy radicals over cage return and cage escape. Additionally, the interpretation of any viscosity effects can become ambiguous if the solvent series used to vary the viscosity significantly influences any of the primary rate constants (such as k_1) other than k_D.[18]

Quantitative relationships describing the behavior of geminate radical pairs as a function of solvent viscosity have been developed, but generally k_{obs} for radical production can be inversely correlated with η or $\eta^{1/2}$.[17] To test for an influence of solvent viscosity on k_{obs}, a plot of k_{obs}^{-1} versus η (Figure 4) was generated using four fluorinated solvents of varying viscosity at temperatures of 20 through 35 °C. Clear linear correlations with nonzero slopes are observed at these temperatures with the viscosity dependence becoming considerably less pronounced at increasing temperatures, with essentially no viscosity dependence at 40 °C. Thus, this behavior suggests that BPPP thermally decomposes by a single-bond homolysis mechanism (Scheme 1a), in contrast to the concerted multiple-bond pathway previously suggested by Zhao.[14] Early studies by Novikov et al.[13] were also suggestive of a single-bond decomposition mechanism as the decomposition of PDPs was observed to increase in the presence of several fluorinated alkenes, presumably due to scavenging of the carboxy radicals from the solvent cage. The decrease in the viscosity dependence on k_{obs} with increasing temperature can most likely be attributed to a very effective competition of k_β at higher temperatures, depleting the carboxy radicals from the solvent cage.

Extrapolation of the k_{obs}^{-1} values to zero viscosity provides semiquantitative information on the intrinsic rate constant for peroxide bond homolysis, k_1, as solvent cage effects should effectively vanish upon approaching gaslike viscosities. Extrapolation yields the zero-viscosity rate constants, k_o, shown in Table 2. These k_o values should be representative of the k_1 values, assuming that viscosity is the primary solvent property influencing changes in the k_{obs} values.

Explanation of the faster k_{obs} values measured for BPPP in CO_2 relative to the fluorinated solvents can be described through consideration of the aforementioned viscosity effects. Figure 5 shows a plot of k_{obs}^{-1} versus viscosity for carbon dioxide at three densities. The correlation of the k_{obs}^{-1} values versus η for carbon dioxide at the three densities investigated agree well with the extrapolated regression of the fluorinated solvents. Normalization of the k_{obs} values for all of the solvents to the appropriate zero-viscosity rate constants, k_o, provides a more useful comparison of the CO_2 data to that of the fluorinated solvents (Table 3). The more viscous fluorinated solvents show k_{obs}/k_o ratios much lower than unity due to pronounced cage effects, with the ratios approaching 1 at higher temperatures. For CO_2, at all densities, the k_{obs} values are very close to the k_o values, suggesting that solvent cage effects are very minimal at these considerably low viscosities. This observation is consistent with other studies of free-radicals and solvent cage effects in carbon dioxide and other low viscosity supercritical fluids.[4,19,20] Indeed, if solvent cage effects are not important in CO_2, the measured k_{obs} values would effectively collapse to be equivalent to k_1. Additionally, the good correlation of viscosity with the k_{obs} values for the fluorinated solvents and CO_2 suggests that other solvent influences such as the dielectric continuum effects observed for AIBN decomposition in CO_2[4] are not operative in the BPPP system and that k_1 is probably similar for all of the solvents.

Table 2. Extrapolated Zero-Viscosity Rate Constants, k_o, from BPPP Decomposition in Fluorinated Solvents

temperature (°C)	$k_o \times 10^5$ (s^{-1})
20	4.91 ± 0.39
25	9.51 ± 0.87
30	14.8 ± 1.4
35	27.2 ± 1.7

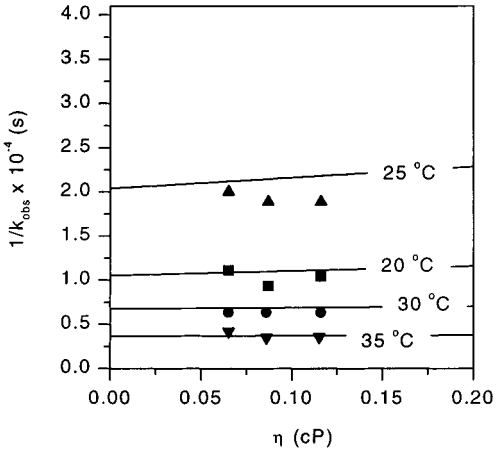

Figure 5. Solvent viscosity and temperature dependence of k_{obs} for BPPP thermal decomposition in carbon dioxide at densities of 0.78, 0.87, and 0.98 g/mL.

Thermal Degradation Product Analysis. Further information regarding the mechanism of diacyl peroxide thermal decomposition can be provided from degradation product analyses. Product formation from BPPP homolysis can originate through radical reactions of **1** (Scheme 1), or **1**-derived radicals, within the initial solvent cage or through diffusive combination. The relative proportion of cage versus diffusion products depends primarily on the radical lifetimes relative to the solvent cage lifetime. Hence, in higher viscosity solvents, the relative concentration of products favored by solvent cage effects usually increases.

On the premise of a single-bond homolysis mechanism, all of the degradation products that could potentially form from

(18) Pryor, W. A.; Smith, K. *J. Am. Chem. Soc.* **1970**, *92*, 5403.

(19) Tanko, J. M.; Suleman, N. K.; Fletcher, B. *J. Am. Chem. Soc.* **1996**, *118*, 11958.

(20) Sigman, M. E.; Leffler, J. E. *J. Org. Chem.* **1987**, *52*, 1165.

Table 3. Rate Constants for BPPP Decomposition in Fluorinated Solvents and Dense Carbon Dioxide Normalized to Extrapolated "Zero-Viscosity" Rate Constants

	k_{obs}/k_o		
solvent	20 °C	25 °C	30 °C
CO_2 (0.78)[a]	1.02 ± 0.08	0.95 ± 0.09	1.07 ± 0.10
CO_2 (0.87)[a]	1.08 ± 0.09	1.13 ± 0.11	1.07 ± 0.11
CO_2 (0.98)[a]	1.08 ± 0.09	1.01 ± 0.09	1.07 ± 0.11
$CFCl_3$	0.85 ± 0.07	0.91 ± 0.09	0.99 ± 0.10
$CF_2ClCFCl_2$	0.69 ± 0.06	0.68 ± 0.08	0.94 ± 0.10
$C_6F_{12}O_2$	0.54 ± 0.05	0.64 ± 0.07	0.66 ± 0.07
$C_{15}F_{30}O_5$	0.25 ± 0.02	0.32 ± 0.03	0.60 ± 0.09

[a] Density in g/mL.

Scheme 2. Potential Radical Coupling and β-Scission Products Which Could Be Formed during the Thermal Decomposition of BPPP

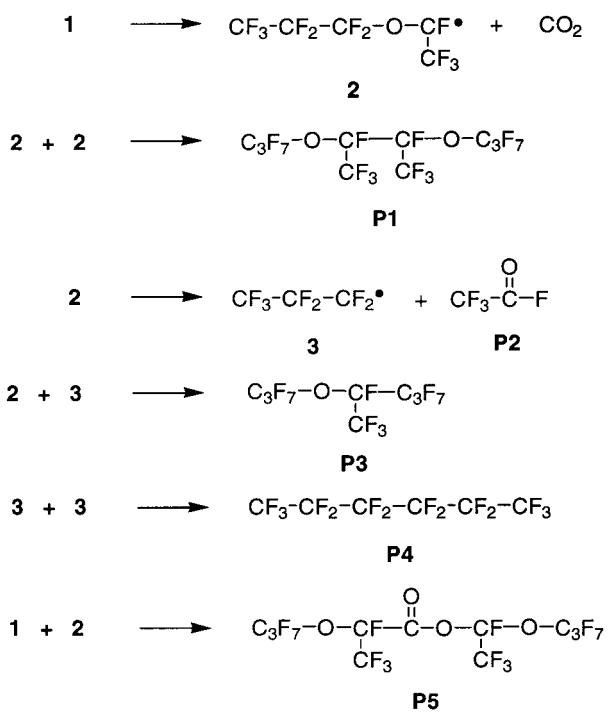

coupling and β-scission reactions of radicals derived from radical **1** are shown in Scheme 2. Product analysis of BPPP decomposed in CO_2, $CF_2ClCFCl_2$, and $C_{15}F_{30}O_5$ at 30 °C was conducted after 48 h through a combination of GC/MS, ^{19}F NMR, and FTIR. For all three of the solvents, the major decomposition product observed was **P1**, derived from coupling of two **2** radicals. Two additional minor products were formed due to the β-scission reaction of radical **2** to form radical **3** and trifluoroacetyl fluoride, **P2**. Coupling of **3** with **2** leads then to **P3**. Formation of **P4** was not detected, most likely due to the relatively small amounts of radical **3** present during the decomposition reaction.

As stated previously, the decomposition products can help to distinguish whether the decomposition mechanism follows a single-bond or multiple-bond pathway. This is possible since in the single-bond pathway, solvent cage reactions can occur, resulting in products which could not form in the multiple-bond pathway (Scheme 3). In the single-bond homolytic decomposition of diacyl peroxides, esters are often obtained as solvent cage products due to radical coupling before complete decarboxylation of the geminate radical pair ($cage_2$, Scheme 3). Unfortunately, the perfluoroester product **P5** was not observed in the decomposition products. One possible reason for this is

Scheme 3. Potential Cage Recombination Reactions in BPPP Decomposition

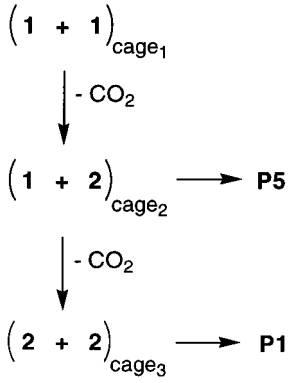

the extreme hydrolytic susceptibility of perfluoroesters.[22] In the method utilized to synthesize these diacyl peroxides, an aqueous biphasic reaction system was typically used. Due to the thermal instability of perfluoroalkyl diacyl peroxides, the synthesis procedure does not typically involve elaborate drying methods, which could result in the presence of trace amounts of water which would catalytically destroy the ester compounds. Even in the most viscous solvent, $C_{15}F_{30}O_5$ (η = 3.8 cP at 30 °C), where cage product formation would be most probable, no spectroscopic evidence of ester formation was found. Due to these reasons, the absence of esters does not necessarily negate their formation.

Radical scavenging experiments conducted in CO_2, $CF_2ClCFCl_2$, and $C_{15}F_{30}O_5$ at 30 °C further suggest a minimal influence of cage recombination reactions on the formation of the major product, **P1**. Addition of CCl_3Br or diethyl ether to the decomposition reactions resulted predominantly in the formation of scavenger-based products ($CF_3CF_2CF_2OCF(CF_3)X$, X = Br or H) with no detectable formation of **P1** in any of the solvents. Therefore, even in the most viscous solvent, practically all of **P1** is formed from random combination of **2** outside of the solvent cage. These results are consistent with the scavenging results of Zhao, which reported greater than 95% of **P1** formed outside of the solvent cage in $CF_2ClCFCl_2$ at 25 °C.[14] The small to nondetectable amount of geminate recombination suggests that BPPP should have a high initiator efficiency for free-radical chain reactions even in relatively high viscosity environments.

Analysis of Activation Parameters for Thermal Decomposition. Further insight into the role of the solvent in the decomposition of BPPP can be gained through analysis of the activation parameters. Analysis of the temperature dependence of k_{obs} in the different solvent systems provided the activation enthalpies ($\Delta H^{\ddagger}$) and activation entropies ($\Delta S^{\ddagger}$) listed in Table 4. Excellent agreement is observed between the activation parameter values for $CF_2ClCFCl_2$ by the FTIR method in this work and those of the iodometric titration method used by Zhao[14] (Table 4). The observed breadth of activation parameter values for BPPP through change of solvent calls into question previously used methods of interpreting activation parameter magnitudes as being indicative of a particular decomposition mechanism.[16] However, a correlation is observed upon examination of the activation parameters: an enthalpy−entropy compensation. This compensation is illustrated more clearly in Figure 6 where a linear correlation between $\Delta H^{\ddagger}$ and $\Delta S^{\ddagger}$ is observed for the different solvents. This type of correlation is

(21) Koenig, T.; Fischer, H. In *Free Radicals*; Kochi, J. K., Ed.; Wiley: New York, 1973; pp 157−189.
(22) DeMarco, R. A.; Couch, D. A.; Shreeve, J. M. *J. Org. Chem.* **1972**, *37*, 3332.

Table 4. Activation Parameters for BPPP Decomposition in Fluorinated Solvents and Dense Carbon Dioxide

solvent	$\Delta H^{\ddagger}$ (kcal·mol^{-1})	$\Delta S^{\ddagger}$ (cal·mol^{-1}·K^{-1})
CO_2 (0.78)[a]	18.6 ± 0.7	−14.5 ± 1.8
CO_2 (0.87)[a]	19.2 ± 0.3	−12.7 ± 1.5
CO_2 (0.98)[a]	20.7 ± 0.4	−7.5 ± 1.3
$CFCl_3$	22.6 ± 0.1	−1.5 ± 0.5
$CF_2ClCFCl_2$	24.1 ± 0.1	3.6 ± 0.2
$CF_2ClCFCl_2$[b]	23.8 ± 0.1	3.1 ± 0.2
$C_6F_{12}O_2$	25.7 ± 0.2	7.8 ± 0.6
$C_{15}F_{30}O_5$	30.9 ± 0.1	24.8 ± 0.2

[a] Density in g/mL. [b] From ref 14.

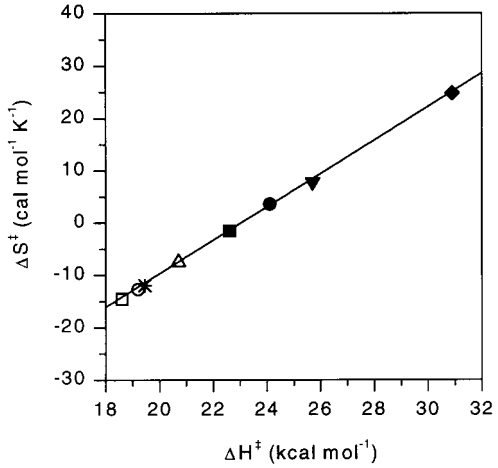

Figure 6. Correlation of activation enthalpy and activation entropy for BPPP decomposition in fluorinated solvents (solid symbols), carbon dioxide (open symbols), and at "zero-viscosity" (star).

often referred to as an *isokinetic relationship* (IKR), suggestive of a linear free-energy relationship in the system. However, such linear correlations between $\Delta H^{\ddagger}$ and $\Delta S^{\ddagger}$ are often merely coincidental and not usually statistically sound.[23]

A truer test of the existence of an IKR can be determined from the Van't Hoff plots. An IKR would result in a convergence of the Van't Hoff lines to a single point referred to as the isokinetic temperature (IKT) where the difference between the rate constants in the series of compared reactions is at a minimum.

Examination of the Van't Hoff plot for the fluorinated solvents (Figure 7) does show a convergence of the lines with a similar intersection point for $CFCl_3$, $CF_2ClCFCl_2$, and $C_6F_{12}O_2$ but with deviation for $C_{15}F_{30}O_5$. A true IKR, if existing in this system, is not inclusive of all the solvents. It has been reported that isosolvent (one reaction carried out in a series of solvents) IKRs are difficult to substantiate and are rarely statistically sound.[24] However, the existence of a IKR on k_1, or any other of the primary rate constants, would be difficult to observe and potentially interpret due to the composite nature of k_{obs}. In fact, the observed compensation effect for k_{obs} may be a result of the complex interplay between the changing k_D for the different solvents as well as the increasing importance of k_β with temperature. This interpretation would be consistent with the observed decreasing importance of viscosity on k_{obs} with temperature leading to essentially identical k_{obs} values for all of the fluorinated solvents at high temperature.

Analysis of the extrapolated k_o values yields the "zero-viscosity" activation parameters of $\Delta H^{\ddagger}_o = 19.5 \pm 0.97$ kcal·mol^{-1} and $\Delta S^{\ddagger}_o = -11.9 \pm 3.2$ cal·mol^{-1}·K^{-1}. If the k_o values are a good estimation of the true k_1 values, then $\Delta H^{\ddagger}_o$ and $\Delta S^{\ddagger}_o$ should be indicative of the intrinsic activation parameters for bond homolysis of BPPP decomposition. Thus, the low $\Delta H^{\ddagger}_o$ should represent the bond-strength of the diacyl peroxide (O−O) bond with the highly negative $\Delta S^{\ddagger}_o$ suggesting a highly ordered transition state for bond breaking. In comparison, the activation parameters with increasing solvent viscosity show an increase in magnitude of $\Delta H^{\ddagger}$ along with a more positive $\Delta S^{\ddagger}$. Thus, as the viscosity increases, a higher effective activation barrier is imposed due to increased diffusive barriers. The increasing positive character of $\Delta S^{\ddagger}$ with increasing solvent viscosity suggests an increasing effective entropic gain for escape of the geminate radical pair from the solvent cage.

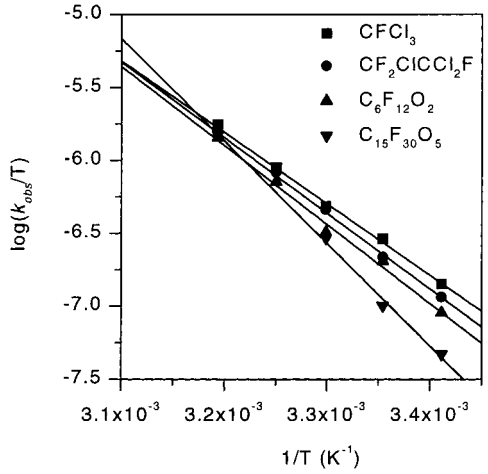

Figure 7. Van't Hoff plot for BPPP decomposition in fluorinated solvents.

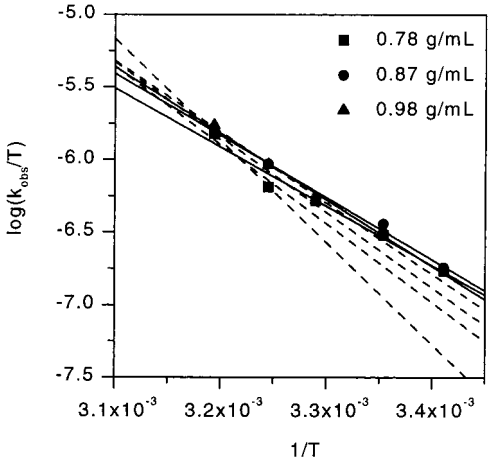

Figure 8. Van't Hoff plot for BPPP decomposition in carbon dioxide. Dashed lines represent linear fits for fluorinated solvents in Figure 7.

Comparison of the Van't Hoff lines for CO_2 (Figure 8) to the fluorinated solvents shows a strong correlation with the convergence behavior of the fluorinated solvents. This convergence behavior of the CO_2 lines along with similarity of the CO_2 activation parameters to that of the zero-viscosity values further suggests that k_1 in CO_2 is similar to the fluorinated solvents. Due to the minimal influence of solvent cage effects in CO_2 other weaker interactions may also be influencing the activation parameters, such as the proposed solvent−solute interactions between CO_2 and fluorinated compounds.[25] However, more detailed studies would have to be conducted to

(23) Linert, W. *Chem. Soc. Rev.* **1994**, *23*, 429.
(24) Linert, W.; Jameson, R. F. *Chem. Soc. Rev.* **1989**, *18*, 477.
(25) Dardin, A.; DeSimone, J. M.; Samulski, E. T. *J. Phys. Chem. B* **1998**, *102*, 1775.

Table 5. Activation Parameters Comparison for Thermal Decomposition of BPPP and TFAP in Different Solvents

	TFAP		BPPP	
	CO_2 (0.87)[a]	$CF_2ClCFCl_2$[b]	CO_2 (0.87)[a]	$CF_2ClCFCl_2$
$\Delta H^{\ddagger}$ (kcal·mol^{-1})	20.8 ± 0.2	25.8	19.2 ± 0.3	24.1 ± 0.1
$\Delta S^{\ddagger}$ (cal·mol^{-1}·K^{-1})	−14.1 ± 1.1	0.7	−12.7 ± 1.5	3.6 ± 0.2
$\Delta G^{\ddagger}$ (kcal·mol^{-1})	25.4	25.6	23.1	23.0

[a] Density in g/mL. [b] Reference 29.

Table 6. Activation Parameters for AP Decomposition in CO_2, the Gas Phase, and Cyclohexane

	CO_2 (0.83)[a]	gas-phase[b]	C_6H_{12}[c]
$\Delta H^{\ddagger}$ (kcal·mol^{-1})	28.5 ± 0.4	28.8	31.4
$\Delta S^{\ddagger}$ (cal·mol^{-1}·K^{-1})	3.1 ± 1.5	4.29	11.0
$\Delta G^{\ddagger}$ (kcal·mol^{-1})	27.4	27.3	27.5

[a] Density in g/mL. [b] Reference 28. [c] Reference 26.

determine the influence, if any, of such interactions on the decomposition kinetics.

Model Compound Studies. To gain further insight into the magnitude of the "intrinsic" activation parameters for BPPP, two additional initiators were investigated: trifluoroacetyl peroxide (TFAP) and acetyl peroxide (AP). TFAP serves as a model compound for PDPs such as BPPP, allowing for comparison of the activation parameter change to that of its nonfluorinated analogue, AP, which has been extensively studied in the literature.[18,26−28] If the k_{obs} value of TFAP and AP can be assumed to approximate their k_1 values due to the low viscosity of CO_2, the activation parameters for TFAP and AP can be directly compared for examination of structural effects.

The utility of TFAP as a model compound for BPPP can be shown by comparison of the activation parameters for each of them in CO_2 and $CF_2ClCFCl_2$ (Table 5). BPPP is thermally more labile than TFAP as indicated by its lower $\Delta G^{\ddagger}$ value, which is consistent with the observed effects of fluoroalkyl chain length on the stability of PDPs.[15] A similar difference in $\Delta H^{\ddagger}$ and $\Delta S^{\ddagger}$ for each initiator upon change in solvent from CO_2 to $CF_2ClCFCl_2$, along with solvent independent $\Delta G^{\ddagger}$ values (compensation effect) are observed with the two initiators. This suggests analogous solvent cage effects are operative in these two initiator systems. Additionally, both BPPP and TFAP possess highly negative $\Delta S^{\ddagger}$ values in CO_2, indicative of highly ordered transition states for bond breaking.

The decomposition of AP has been extensively studied in solvents[18,26] and the gas-phase,[28] exhibiting decomposition via a single-bond homolysis mechanism. Table 6 gives a comparison of the activation parameters measured for CO_2 in this work to that of literature values for the gas-phase[28] and cyclohexane.[26] The activation parameters for CO_2 match well with that of the gas-phase values but differ from that for cyclohexane. The agreement between the gas-phase and CO_2 activation parameters supports the idea that k_{obs} is representative of k_1 at CO_2's gaslike viscosities. The dissimilar $\Delta H^{\ddagger}$ and $\Delta S^{\ddagger}$ values for cyclohexane accompanied with the identical $\Delta G^{\ddagger}$ values for the three media are consistent with the compensation effects of a higher viscosity solvent.

Comparison of the activation parameters for TFAP (Table 5) to that of AP (Table 6) in CO_2 yields several noticeable differences. In comparison, $\Delta G^{\ddagger}$ is lower for TFAP than AP, which is consistent with previous observations.[29] Examination of the $\Delta S^{\ddagger}$ values suggests that the transition state for bond-breaking is considerably more ordered for TFAP than AP. The reason fluorinated diacyl peroxides would have a more ordered transition state than the nonfluorinated analogues is unclear and warrants further structural studies. Indeed, CO_2 is an ideal solvent for these studies due to its seemingly minimal intervention in the decomposition of these initiators through solvent cage effects.

Conclusions

The mechanism and kinetics of the thermal decomposition of the perfluoroalkyl diacyl peroxide, BPPP, was studied through solvent variation and decomposition product analysis. A single-bond homolysis mechanism was determined for the initiator through analysis of the viscosity dependence on k_{obs}. The k_{obs} values for carbon dioxide were similar to the extrapolated "zero-viscosity" rate constants, suggesting the absence of any significant solvent cage effects in the low-viscosity medium. These results additionally suggest that k_1 for bond homolysis in CO_2 is similar to that of the fluorinated solvents. Additional decomposition studies of TFAP and AP in CO_2 further support a lack of solvent cage effects on diacyl peroxide decomposition in CO_2.

Experimental Section

Materials. All solvents and reagents were used as received. SFE/SFC grade carbon dioxide was supplied by Air Products and Chemicals Inc. Galden DET (MW 400) and Galden D03 (MW 867), which are low-molecular weight perfluoropolyethers of the structure (CF_3[(OCF(CF_3)CF_2)$_n$-(OCF_2)$_m$]OCF_3), and referred to subsequently by the following average structures, $C_6F_{12}O_2$ and $C_{15}F_{30}O_5$, respectively, were purchased from Lancaster. Fluorotrichloromethane ($CFCl_3$), 1,1,2-trichlorotrifluoroethane ($CF_2ClCFCl_2$), and trichloromethyl bromide (CCl_3Br) were purchased from Aldrich Chemical Co. Perfluoro-2-*N*-propoxypropionyl fluoride was kindly provided by DuPont.

Synthesis of Diacyl Peroxide Initiators. Bis(perfluoro-2-*N*-propoxypropionyl) peroxide (BPPP) was synthesized by the procedure of Zhao[14] through the heterogeneous reaction of a 1:2 aqueous hydrogen peroxide:potassium hydroxide solution with perfluoro-2-*N*-propoxypropionyl fluoride dissolved in an appropriate fluorinated solvent at low tempeature. After drying with sodium sulfate and determination of the active peroxide concentration through iodometric titration, the BPPP solutions were stored at −78 °C. Trifluoroacetyl peroxide (TFAP) and acetyl peroxide (AP) were synthesized by similar means using the corresponding anhydrides.[29]

Characterization. ^{19}F NMR spectra were obtained at 376.21 MHz with a Varian XL 400 spectrometer, with chemical shift values externally referenced to $CFCl_3$. Mass spectra were obtained on a HP 5985B GC/MS equipped with a J&W GS-Q 30 m × 0.32 mm widebore capillary column in both CI (methane) and EI (70 eV) modes.

Thermal Decomposition Kinetics Experiments in Fluorinated Solvents. All FTIR spectra were recorded on a Bio-Rad FTIR spectrometer with the data processed using the Win-IR software package. The kinetics experiments were conducted in an in-house built high-pressure, variable-temperature optical cell which utilized CaF_2 windows and spacers (Corning, Inc.) to allow for an approximate 1 mm optical path length.

(26) Levy, M.; Steinberg, M.; Szwarc, M. *J. Am. Chem. Soc.* **1954**, *76*, 5978.
(27) Levy, M.; Szwarc, M. *J. Am. Chem. Soc.* **1954**, *76*, 5981.
(28) Renbaum, A.; Szwarc, M. *J. Am. Chem. Soc.* **1954**, *76*, 5975.
(29) Sawada, H.; Nakayama, M. *J. Fluor. Chem.* **1990**, *46*, 423.

For decomposition studies in the fluorinated solvents the diacyl peroxides were synthesized directly in the appropriate solvents and diluted to experimentally appropriate concentrations. For a typical experiment, a small aliquot of the peroxide was degassed through a series of four to five freeze−pump−thaw cycles followed by blanketing under an argon atmosphere. Prior to injection of the initiator solution, the high-pressure optical cell was purged with argon for ca. 30 min. Once the temperature of the optical cell stabilized at the desired temperature, the peroxide solution was injected into the cell against a positive argon purge and then sealed. Spectra were collected at constant time intervals, depending on the reaction temperature: 900 s at 20 °C, 600 s at 30 °C, and 300 s at 40 °C. After 24 h and complete peroxide decomposition, a final spectrum was collected and used as the background spectrum in the analysis of the kinetic data.

FT-IR difference spectra were used to calculate the relative change in concentration of peroxides as a function of time. These spectra were obtained by subtracting the reaction spectra at 24 h (complete decomposition) from the collected absorbance spectra thereby eliminating all constant absorbances due to the reaction medium. The relative changes in peroxide concentration with time were calculated from the difference absorbance spectra using a curve-fitting program in the Win-IR software package.

Thermal Decomposition Kinetics Experiments in Carbon Dioxide. For the decomposition experiments in carbon dioxide, the procedure for the fluorinated solvents was slightly modified. Approximately 200 μL of a relatively concentrated, degassed solution of the diacyl peroxide in $CF_2ClCFCl_2$ was injected into the degassed, thermally equilibrated optical cell under an argon cross-purge. The cell was pressurized with the CO_2 to the desired pressure using an ISCO 240D syringe pump and then sealed. All other aspects of the decomposition kinetics procedure were similar to that of the fluorinated solvents.

Decomposition Product Analyses. The decomposition of BPPP was carried out at 30 °C in CO_2 (0.78−1.0 g/mL), $CF_2ClCFCl_2$, and $C_{15}F_{30}O_5$, and left for 48 h to ensure complete decomposition. GC/MS along with ^{19}F NMR were used to verify product structures.

$[CF^a_3CF^b_2CF^c_2OCF^d(CF^e_3)]_2$: ^{19}F NMR δ 82.0 (s, 3F, a), 130.5 (m, 2F, b), 82.1 (d, 2F, c), 140.3, 142.1 (d, 1F, d), 78.0, 79.2 (d, 3F, e); CI-MS *m*/*e* 551($M^+ - 19$), 385, 335, 285, 263, 219, 197, 169, 150, 147, 119, 100, 97, 69, 50

CF_3CFO: CI-MS *m*/*e* 116(M^+), 97, 69, 50, 47

CF_3CF_2CFO: CI-MS *m*/*e* 166(M^+), 147, 119, 69, 50, 47

$CF_3CF_2CF_2OCF(CF_3)CFO$: CI-MS *m*/*e* 313($M^+ - 19$), 285, 247, 219, 197, 169, 147, 131, 119, 100, 97, 69, 50, 47

$CF_3CF_2CF_2OCF(CF_3)CF_2CF_2CF_3$: CI-MS *m*/*e* 385($M^+ - 69$), 363, 285, 263, 219, 197, 169, 147, 131, 119, 100, 97

Radical Scavenger Experiments. The thermal decomposition of BPPP at 30 °C in CO_2 (0.78−1.0 g/mL) and $CF_2ClCFCl_2$ was performed with the addition of the radical scavenger, CCl_3Br. As reported by Zhao et al.,[14] a 5 mol equiv excess of scavenger was used to ensure maximum radical-scavenging efficiency. ^{19}F NMR analysis of both systems indicated the predominant scavenged product to be $CF_3CF_2CF_2OCF(CF_3)Br$.

$CF^a_3CF^b_2CF^c_2OCF^d(CF^e_3)Br$: ^{19}F NMR δ 81.9 (s, 3F, a), 130.4 (s, 2F, b), 85.6 (m, 2F, c, $J_{AB} = 1279$ Hz), 77.6 (m, 1F, d), 85.3 (s, 3F, e).

As CCl_3Br was immiscible with $C_{15}F_{30}O_5$, the use of diethyl ether as the scavenger was required.

Acknowledgment. We gratefully acknowledge support through the National Science Foundation Science and Technology Center (CHE-9876674), the EPA for an NCERQA STAR fellowship to W.C.B., and the Alfred P. Sloan Foundation.

JA0103344